Table 1. Paleomagnetic results by site. The positions of paleomagnetic sites are indicated in centimeters (Fig. 4). Sites are classified according to Johnson's system (16): class 1 if precision parameter k (15) was greater than 10, class 2 if k was less than 10, and class 3 if one specimen was used.

Site	Height (cm)	Mean declination (degrees)	Inclination (degrees)	VGP latitude (degrees)	VGP longitude (degrees E)	Class	Lithology
TDS7	1408	353	55	81	218	1	Red silt
TDS5	1352	311	79	53	329	2	Red silt
TDS6	1279	9	69	78	24	3	Red silt
TDS4	1205	25	54	69	100	3	Red silt
TDS3	1190	358	66	84	344	1	Bat guano
TDN18	930	130	61	6	31	2	Carbonated silt
TDN17	880	184	−14	−55	350	1	Carbonated silt
TDN15	815	168	−44	−71	31	2	Carbonated silt
TDN14	750	204	−32	−58	310	3	Red silt
TDN12	617	250	−71	−44	225	3	Red silt
TDN7	615	202	−29	−57	315	2	Red silt
TDN13	445	196	−65	−78	239	1	Red silt
TDN11	435	195	−55	−76	292	1	Red sandy silt
TDN10	320	202	−53	−71	286	3	Red sandy silt
TDN8	235	196	−55	−76	290	1	Speleothem
TDN9	230	180	−56	−84	356	3	Speleothem
TDS2	150	250	−23	−23	271	1	Yellow silt
TDS1	110	108	−2	−14	75	1	Yellow silt
TDN4	35	233	−29	−37	280	3	Red clay
TDN2	30	187	−11	−53	345	2	Red clay
TDN1	17	264	−56	−28	240	2	Red clay
TDN3	15	250	−56	−37	248	2	Red clay

Unconformities are likely in karst environments. On the other hand, we cannot rule out the possibility that the Gran Dolina sediments with reverse magnetization are younger than Jaramillo. If that is the case, then a rough sedimentation rate of about 50 cm per 1000 years is indicated; this value is consistent with the rates of deposition found in other cave sediments (12). The stratigraphic level TD6, and hence the Aurora stratum, is located within Matuyama and therefore is older than 0.78 Ma.

REFERENCES AND NOTES

1. E. Carbonell and X. P. Rodriguez, J. Hum. Evol. 26, 291 (1994).
2. J.-L. Arsuaga, I. Martínez, A. Gracia, J.-M. Carretero, E. Carbonell, Nature 362, 534 (1993) and references therein.
3. J. C. Carracedo, F. Heller, V. Soler, E. Aguirre, in (13), pp. 193–199.
4. Clay and silt deposits are sufficiently soft and contain an appreciable amount of water such that samples were obtained by simply hammering a brass tube with a stainless steel reinforced tip that was pushed into the cleaned outcrop surface at any desired angle. A standard orientation device (compass-inclinometer) was used to measure the azimuth and dip of the obtained cylinders in situ. Sediment samples were stored in cylindrical plastic boxes and were impregnated with a water solution of sodium silicate (1:1) to prevent further distortion. For harder deposits (lithified siltstones and speleothems), a portable drill fitted with a diamond coring bit (diameter 2.5 cm) was used to obtain the samples in the field.
5. E. Carbonell et al., Science 269, 826 (1995).
6. Magnetization measurements were made on a GM400 three-axis SQUID magnetometer housed in a three-pair Helmholtz coil at CSIC in Barcelona. The noise level of this magnetometer is 7×10^{-3} mA m^{-1}, well below the magnetization intensity of the measured samples. Least-squares fits to the linear demagnetization trajectories for both the low- and high-temperature components in each sample were made by principal components analysis [J. L. Kirschvink, Geophys. J. R. Astron. Soc. 62, 699 (1980)].
7. D. Suk, D. R. Peacor, R. Van der Voo, Nature 345, 611 (1990).
8. R. Grun and E. Aguirre, in (13), pp. 201–204.
9. S. C. Cande and D. Kent, J. Geophys. Res. 97, 13917 (1992).
10. O. Oms et al., Phys. Earth Planet. Inter. 85, 173 (1994).
11. J.-P. Valet and L. Meynadier, Nature 366, 234 (1993).
12. V. A. Schmidt, Science 217, 827 (1982); R. Lovlie, K. L. Ellingsen, S.-E. Lauritzen, Geophys. J. Int. 120, 499 (1995).
13. E. Aguirre, E. Carbonell, J. M. Bermúdez de Castro, Eds., El hombre fósil de Ibeas y el Pleistoceno de la Sierra de Atapuerca (Junta de Castilla y León, Valladolid, Spain, 1987).
14. J. D. A. Zijderveld, in Methods in Palaeomagnetism, D. W. Collinson, K. M. Creer, S. K. Runcorn, Eds. (Elsevier, Amsterdam, 1967), pp. 254–286.
15. R. A. Fisher, Proc. R. Soc. London Ser. A 217, 295 (1953).
16. N. M. Johnson et al., J. Geol. 93, 27 (1985).
17. We thank J. Bischoff, W. J. Glen, W. Farrand, J. Stamatakos, R. Van der Voo, and two anonymous reviewers for discussion and J. Dinarès and A. Gómez for laboratory assistance. The excavations were supported by funds from Dirección General de Investigación Científica y Técnica (DGICYT; project PB93066C3-03) and Junta de Castilla y León. Laboratory measurements were supported in part by DGICYT (project PB91-0096).

Functional Significance of Symmetrical Versus Asymmetrical GroEL-GroES Chaperonin Complexes

Andreas Engel,* Manajit K. Hayer-Hartl, Kenneth N. Goldie, Günter Pfeifer, Reiner Hegerl, Shirley Müller, Ana C. R. da Silva, Wolfgang Baumeister, F. Ulrich Hartl

The Escherichia coli chaperonin GroEL and its regulator GroES are thought to mediate adenosine triphosphate–dependent protein folding as an asymmetrical complex, with substrate protein bound within the GroEL cylinder. In contrast, a symmetrical complex formed between one GroEL and two GroES oligomers, with substrate protein binding to the outer surface of GroEL, was recently proposed to be the functional chaperonin unit. Electron microscopic and biochemical analyses have now shown that unphysiologically high magnesium concentrations and increased pH are required to assemble symmetrical complexes, the formation of which precludes the association of unfolded polypeptide. Thus, the functional significance of GroEL:(GroES)$_2$ particles remains to be demonstrated.

Chaperonins mediate the adenosine triphosphate (ATP)–dependent folding of newly synthesized proteins in the cytosol, in mitochondria, and in chloroplasts (1), preventing off-pathway steps during folding that result in aggregation. This function is intimately connected with the characteristic oligomeric structure of chaperonins, which has been analyzed by electron microscopy (2–5) and x-ray crystallography (6). The chaperonin of E. coli, GroEL, is composed of 14 subunits that are arranged in two heptameric rings stacked back-to-back, resulting in a cylindrical structure enclosing a central cavity. Three domains are distinguishable in the 58-kD subunit (6): (i) an equatorial domain that mediates the contact between the rings and contains the ATP binding site, (ii) an apical domain that forms the opening of the central cavity, and (iii) an intermediate, hinge domain. Electron microscopic data

A. Engel, K. N. Goldie, S. Müller, Maurice E. Müller Institute, Biozentrum, University of Basel, CH-4056 Basel, Switzerland.
M. K. Hayer-Hartl, A. C. R. Silva, F. U. Hartl, Howard Hughes Medical Institute and Cellular Biochemistry and Biophysics Program, Memorial Sloan-Kettering Cancer Center, New York, NY 10021, USA.
G. Pfeifer, R. Hegerl, W. Baumeister, Max Planck Institut für Biochemie, D-82150 Martinsried, Germany.

*To whom correspondence should be addressed.

have suggested that unfolded polypeptide substrates bind within the GroEL cylinder at the level of the apical domains (4, 5, 7), which expose a putative hydrophobic binding surface toward the cavity (8).

Folding occurs through ATP hydrolysis–dependent cycles of protein release from the chaperonin followed by rebinding. This process is regulated by the interaction of GroEL with GroES, a single heptameric ring of ~10-kD subunits that coordinates ATP hydrolysis and protein folding (9, 10). A flexible loop region in GroES mediates its nucleotide-dependent association with GroEL (11), which results in inhibition of the GroEL adenosine triphosphatase (ATPase) (9, 12–14). Optimum folding activity and ATPase inhibition are achieved at a 1:1 stoichiometry of GroEL tetradecamers to GroES heptamers (4, 9, 10, 14–16). Together with the results of biochemical analysis of the chaperonin ATPase cycle (10, 14, 17), this observation indicates that the functional chaperonin unit is asymmetrical, providing for the accessibility of the GroEL cavity to substrate polypeptide at all times. Indeed, the formation of chaperonin complexes with a single ring of GroES bound to one end of the GroEL cylinder has been demonstrated by electron microscopy (3–5, 18). In contrast, the recent observation of GroEL:(GroES)$_2$ complexes, with GroES heptamers bound coaxially at both ends of

the GroEL cylinder (15, 19, 20), has suggested a markedly different mechanism of chaperonin action. In this model, the binding and folding of substrate polypeptides are proposed to occur exclusively at the outer GroEL surface (15).
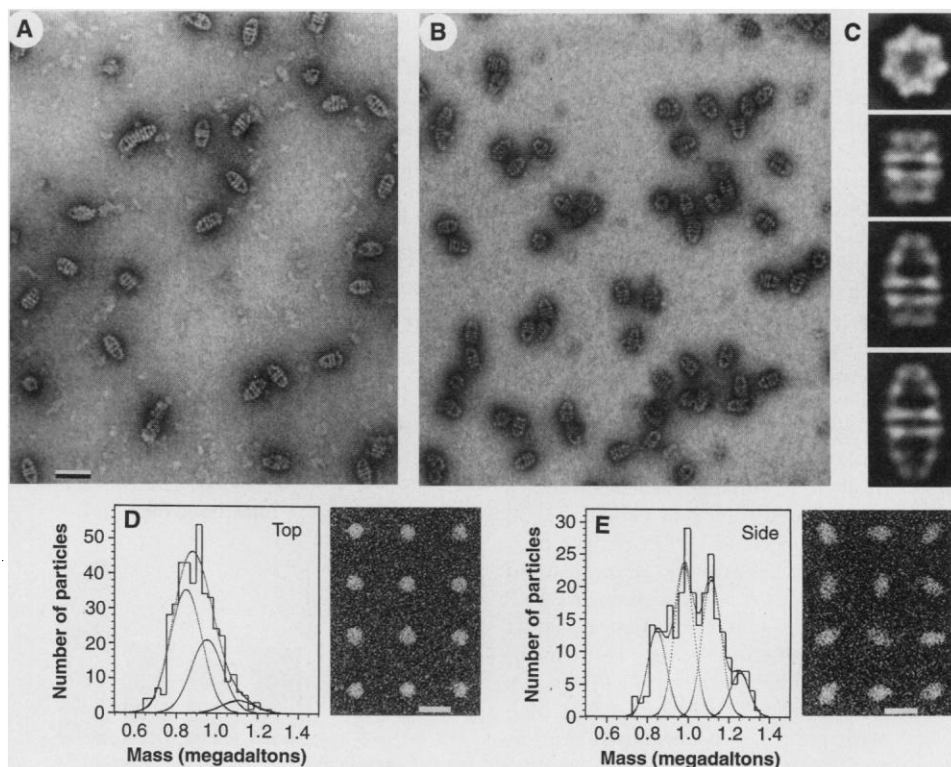
We have now analyzed the requirements for the formation of asymmetrical and sym-

metrical chaperonin complexes. The ratio of asymmetrical to symmetrical complexes under different conditions is often assessed by visualizing mixtures of GroEL and GroES by negative staining with uranyl salts (2–4, 15, 18–20). We followed this approach by incubating GroEL and GroES in the presence of ATP or adenosine diphosphate (ADP), un-

Table 1. Statistical analysis of negatively stained chaperonin complexes detected by electron microscopy. Incubation of GroEL and GroES, cross-linking, and staining were performed as in Fig. 1 with the following buffer conditions: A, 50 mM tris-HCl (pH 8.0), 50 mM KCl, 50 mM MgCl$_2$; and B, 20 mM MOPS-KOH (pH 7.2), 50 mM KCl, and 5 mM MgCl$_2$. ATP (2.5 mM), 2.5 mM ADP, 2.5 mM AMP-PNP, or 2.5 mM AMP-PNP plus 0.3 μM 6His-N-DHFR [substrate protein (S)] were present as indicated. For the latter condition, GroEL was incubated with 6His-N-DHFR before addition of GroES and AMP-PNP, as in Fig. 2B. Data sets marked by an asterisk were obtained by digital image processing and classification from images such as those shown in Fig. 1. Particle populations selected manually were angularly and translationally aligned, and normalized. They were subsequently submitted to a multivariate statistical classification, partitioning particles into classes according to their structural similarity (22). A(ATP) and A(ADP) resulted from visual interpretation of data sets A(ATP)* and A(ADP)*, respectively. All other entries are from particles recorded with a fixed-beam transmission electron microscope after visual particle classification.

Condition	Unclass-ified (%)	Top views (%)	Side views (%)			Particles analyzed
			GroEL	GroEL: GroES	GroEL: (GroES)$_2$	
A(ATP)*	13*	12*	2*	31*	42*	1087*
A(ATP)	20	9	3	29	39	1087
A(ADP)*	5*	6*	0*	89*	0*	536*
A(ADP)	11	9	1	76	3	536
A(AMP-PNP)	18	12	0	11	59	234
A(AMP-PNP)(S)	17	21	0	60	2	920
B(ATP)	25	37	2	33	3	709

Fig. 1. Negatively stained and freeze-dried chaperonin particles detected by scanning transmission electron microscopy (STEM). (**A** and **B**) A mixture of 0.12 μM GroEL oligomer and 0.6 μM GroES oligomer was incubated for 15 min at 25°C in 50 mM tris-HCl (pH 8.0), 50 mM KCl, 50 mM MgCl$_2$, and either 2.5 mM ATP (A) or 2.5 mM ADP (B), cross-linked for 15 min at 25°C in 0.1% glutaraldehyde, adsorbed to carbon film, and stained with uranyl formate (33). GroEL and GroES were isolated as described previously (4, 10, 14). Concentrations were determined by quantitative amino acid analysis. (**C**) Averages of the characteristic projections resulting from the multivariate statistical analysis of 477 chaperonin particles (22). From top to bottom: top view, GroEL side view, GroEL: GroES side view, and GroEL:(GroES)$_2$ side view. The relative occurrence of the projections is given in Table 1. (**D** and **E**) Top views and side views, respectively, of freeze-dried unstained GroEL-GroES complexes assembled and cross-linked as in (A) were recorded for mass evaluation at a dose of 200 to 400 electrons per square nanometer with a Vacuum Generators STEM HB5 operated at 80 kV (right panels) (23). (D, left panel) Mass histogram from 404 top views with two Gaussian peaks fitted at 850 and 950 kD, representing GroEL and GroEL:GroES complexes, respectively. The minor peak at 1100 kD may be the result of a few symmetrical GroEL-GroES particles viewed along their cylinder axis. (E, left panel) Mass histogram from 382 side views with three major Gaussian peaks fitted at 850, 950, and 1120 kD, representing GroEL, GroEL:GroES, and GroEL:(GroES)$_2$ complexes, respectively. The fourth, minor peak probably represents sym-

metrical GroEL-GroES particles with one additional GroES ring. Mass analysis and Gaussian peak fitting were performed as described (23). Scale bars, 20 nm.

der conditions that favor the formation of either GroEL:(GroES)$_2$ (Fig. 1A) or GroEL:GroES (Fig. 1B) complexes, respectively (20). The interaction between GroEL and GroES was stabilized by glutaraldehyde cross-linking (15, 21). Consistent with previous observations (3–5, 18–20), four types of particles were detected, as shown by the averaged images in Fig. 1C: top views with a sevenfold rotational symmetry and side views exhibiting the three characteristic morphologies of GroEL ("bricks"), GroEL:GroES ("bullets"), and GroEL:(GroES)$_2$ ("footballs"). The respective populations were determined either by a multivariate statistical analysis (22) or by visual inspection (Table 1).

In end-on projections, the two types of GroEL-GroES complexes were indistinguishable from each other or from free GroEL. We therefore used a scanning transmission electron microscope (STEM) (23) to determine the mass of freeze-dried, unstained chaperonin particles assembled under conditions promoting the formation of GroEL:(GroES)$_2$ structures (20). Because top and side views of the complexes could be discerned in low-dose STEM dark-field micrographs (Fig. 1, D and E), their respective masses could be measured. The mass histograms show that top views contained at most 6% GroEL:(GroES)$_2$ complexes (Fig. 1D), whereas side views comprised 20% GroEL tetradecamers, 36% GroEL:GroES, and 33% GroEL:(GroES)$_2$ particles (Fig. 1E). Thus, measurements of particle populations from negatively stained samples, based exclusively on the evaluation of side projections, may overestimate the abundance of symmetrical complexes. Top views represented the major fraction ($\geq$70%) of particles in micrographs that were used for a quantitative analysis of the occurrence of GroEL, GroEL:GroES, and GroEL:(GroES)$_2$ complexes (20).

The analysis of negatively stained GroEL particles in conjunction with the mass measurements allowed us to define the experimental conditions that favor the formation of symmetrical and asymmetrical chaperonin complexes (Table 1). Significant populations of GroEL:(GroES)$_2$ structures were detected only in the presence of ATP [or the nonhydrolyzable analog adenylyl-imidodiphosphate (AMP-PNP)] at pH 8.0 and 50 mM Mg^{2+} (20) (Table 1). GroEL:(GroES)$_2$ structures were essentially absent when GroEL and GroES were incubated with ATP in 5 mM Mg^{2+} at pH 7.2, that is, under conditions previously used to obtain maximal protein folding activity (4) (Table 1). Combining low Mg^{2+} with pH 8.0 or high Mg^{2+} with pH 7.2 also minimized the formation of symmetrical complexes (see below). Although the chaperonin system is functional in protein folding under all of these conditions, folding is more efficient at

low Mg^{2+} concentrations and pH 7.2 (24). In agreement with previous studies, only asymmetrical GroEL:GroES complexes were detected on incubation with ADP and Mg^{2+} (4, 15, 20), even in buffers that allow the assembly of symmetrical particles in the presence of ATP (Table 1).

To test the validity of the electron microscopic analysis of chaperonin complexes, we established reliable biochemical binding assays capable of distinguishing between GroEL:GroES and GroEL:(GroES)$_2$ particles. Removal of free GroES by size-exclusion chromatography results in the dissociation of symmetrical complexes to asymmetrical complexes (20), suggesting that one of the two GroES oligomers is less stably bound, at least in the presence of ATP. This conclusion is consistent with the observation that, under the appropriate buffer conditions, high concentrations of ATP ($\sim$400 μM) are necessary for halfmaximal formation of GroEL:(GroES)$_2$ complexes, whereas much lower concentrations of ATP are sufficient for the halfmaximal formation of GroEL:GroES particles (15) and for GroEL- and GroES-dependent protein folding (24). To avoid separation of GroEL:(GroES)$_2$ from free GroES, we initially analyzed the interaction between the two proteins by equilibrium dial-

ysis with [^{3}H]GroES (25). As expected, in the presence of ADP, GroES bound to GroEL with 1:1 stoichiometry both at 5 mM Mg^{2+} (pH 7.2) and at 50 mM Mg^{2+} (pH 8.0) (Fig. 2, A and B). Because of the long incubation times, the use of ATP was not practical in these experiments and was therefore substituted by AMP-PNP, which also supports the formation of GroEL:(GroES)$_2$ complexes (15, 20). On incubation with AMP-PNP, binding of GroES to GroEL at a stoichiometry close to 2:1 was observed. However, such 2:1 binding occurred only at the high Mg^{2+} concentration and at pH 8.0 (20) (Fig. 2, B and C). Electron microscopy confirmed that, under these conditions, >70% of the particles in side-orientation represent GroEL:(GroES)$_2$ complexes (Table 1). Thus, conditions favoring the formation of GroEL:(GroES)$_2$ particles reduce the negative cooperative effect normally transduced from the GroES-bound toroid of GroEL to the opposite toroid (4), allowing the two toroids to function independently. Negative cooperativity is apparently most pronounced in the presence of ADP and is then sufficient to suppress the binding of a second GroES oligomer even at high concentrations of Mg^{2+} and at increased pH. Consistent with this observation, the addition of a low ADP concentra-
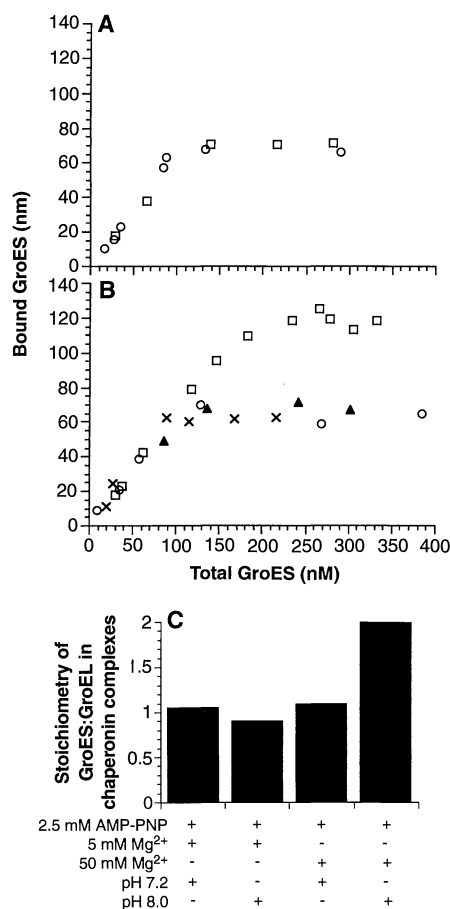

Fig. 2. Analysis of the interaction between GroEL and GroES by equilibrium dialysis. (**A**) GroEL oligomer (60 nM) was incubated with various concentrations of [^{3}H]GroES (4, 27) in buffer A [20 mM MOPS-KOH (pH 7.2), 100 mM KCl, 5 mM magnesium acetate] containing 0.2 mM ADP (○) or 2.5 mM AMP-PNP (□). (**B**) GroEL oligomer (60 nM) was incubated with various concentrations of [^{3}H]GroES in buffer B [50 mM tris-HCl (pH 8.0), 50 mM KCl, 50 mM magnesium acetate] containing 0.2 mM ADP (○), 2.5 mM AMP-PNP (□), 0.2 mM ADP plus 2.5 mM AMP-PNP (▲), or 2.5 mM AMP-PNP plus 120 nM 6His-N-DHFR (✕) (5). (**C**) Stoichiometry of GroES to GroEL in chaperonin complexes determined as in (A) and (B) under the conditions indicated. Equilibrium dialysis was performed in 2-ml units (Spectrum) containing two 1-ml cells separated by a membrane with a 300-kD cutoff. GroEL was added to one cell and [^{3}H]GroES was added to both cells at the concentrations indicated. After 5 hours at 25°C, portions of the contents of each cell were analyzed by scintillation spectroscopy and SDS–polyacrylamide gel electrophoresis. In the absence of added nucleotide, GroEL bound ~5 nM [^{3}H]GroES. This binding was considered nonspecific and was subtracted. When present, 6His-N-DHFR (28) was first incubated with GroEL for 5 min in the absence of nucleotide. The 6His-N-DHFR:GroEL complex was then added to one cell of the dialysis apparatus followed by the addition of AMP-PNP and [^{3}H]GroES to both cells.

tion (0.2 mM) in the presence of 2.5 mM AMP-PNP was sufficient to convert the stoichiometry of GroES binding to GroEL from 2:1 to 1:1 (Fig. 2B). Symmetrical chaperonin complexes may thus exist only when the subunits of both GroEL toroids have ATP or AMP-PNP bound. This situation does not occur in the normal chaperonin ATPase cycle, in which the two toroids are maintained in different nucleotide-bound states, reflecting a structural and functional asymmetry in the double ring (26, 27).
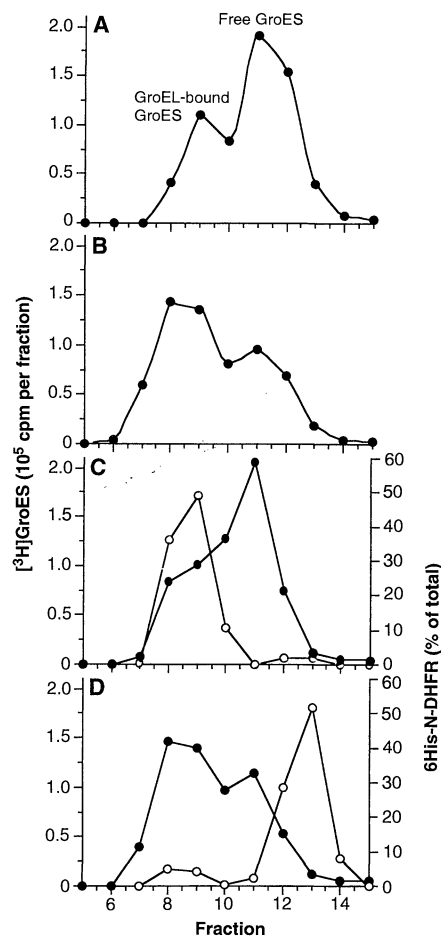

Fig. 3. Analysis of the interaction between GroEL and GroES by size-exclusion chromatography. GroEL (0.5 μM) was incubated for 10 min at 25°C in buffer B containing either 0.2 mM ADP (**A**), 2.5 mM AMP-PNP (**B**) or 2.5 mM AMP-PNP and 0.6 μM 6His-N-DHFR (**C**). [³H]GroES (1.5 μM) was then added for another 10 min. (**D**) GroEL and [³H]GroES were first incubated in buffer B containing 2.5 mM AMP-PNP for 10 min, after which 0.6 μM 6His-N-DHFR was added for another 10 min. The reaction mixtures were subsequently separated on Sephacryl S-300 columns (0.5 by 10 cm) that had been equilibrated with buffer B containing the respective nucleotide. Fractions (150 μl) were collected and analyzed by scintillation spectroscopy and SDS–polyacrylamide gel electrophoresis with Coomassie blue staining. The distribution profiles of [³H]GroES (●) are shown in (A) to (D) and the profiles of 6His-N-DHFR (○) in (C) and (D).

The availability of a biochemical binding assay also allowed us to address the question of whether the GroEL:(GroES)$_2$ complex can form in the presence of unfolded polypeptide. A derivative of mouse dihydrofolate reductase (DHFR) with a 15–amino acid extension, including a six-histidinyl tag, at its NH_2-terminus was chosen as the substrate protein (28). Although monomeric and enzymatically active in the absence of chaperonin, the DHFR moiety in the 6His-N-DHFR derivative was structurally destabilized and bound avidly to GroEL without the need for prior unfolding in denaturant. The interaction with the chaperonin was only prevented in the presence of hydrolyzable ATP and the folate antagonist methotrexate, which stabilizes the native state of DHFR. When 6His-N-DHFR was added to GroEL at a twofold molar excess at 50 mM Mg^{2+} and pH 8.0, subsequent addition of GroES and AMP-PNP did not result in the formation of GroEL:(GroES)$_2$ complexes. Only 1:1 binding of GroES to GroEL was observed by equilibrium dialysis (Fig. 2B). The same result was obtained when unfolded bovine rhodanese was bound to GroEL by dilution from denaturant (29). Electron microscopy confirmed these observations: Only 2% of negatively stained chaperonin complexes could be identified as symmetrical GroEL:(GroES)$_2$ particles when GroEL had substrate protein bound (Table 1) (30).

The saturability of GroEL with two GroES oligomers observed in AMP-PNP–containing buffer (Fig. 2) prompted us to test the stability of the symmetrical complexes. Separation of free GroES from GroEL by size-exclusion chromatography demonstrated that both the GroEL:GroES complexes formed in the presence of ADP (Fig. 3A) and the GroEL:(GroES)$_2$ complexes formed with AMP-PNP at 50 mM Mg^{2+} and pH 8.0 (Fig. 3B) were sufficiently stable to allow isolation. Again, preincubation of GroEL with 6His-N-DHFR reduced the stoichiometry of GroES binding to GroEL from 2:1 to 1:1 (Fig. 3C) (30). However, the initial formation of GroEL:(GroES)$_2$ complexes in the presence of AMP-PNP precluded the association of 6His-N-DHFR with GroEL (Fig. 3D). Thus, unfolded polypeptide likely binds within the central cavity of the chaperonin cylinder.

With the use of electron microscopic and biochemical binding assays, we have shown that symmetrical GroEL:(GroES)$_2$ complexes form in the presence of ATP or AMP-PNP, but only at concentrations of free Mg^{2+} unlikely to occur in cells and at alkaline pH. Mixtures of asymmetrical and symmetrical chaperonin complexes at varying ratios were observed over Mg^{2+} concentrations ranging from 15 to 50 mM and at pH values of 7.5 to 8.0 (31). The concentration of free Mg^{2+} in the E. coli cytosol is only 1 to 2 mM (32). Thus, the conditions required

for the formation of GroEL:(GroES)$_2$ particles are unrelated to the function of GroEL and GroES in protein folding, which is fully efficient at physiological concentrations of free Mg^{2+} and pH 7.2, conditions under which GroEL:(GroES)$_2$ particles do not form. Moreover, when the central cavity of GroEL was obstructed by the association of two GroES oligomers, binding of substrate protein was prevented. On the other hand, binding of polypeptide to GroEL still allowed the formation of asymmetrical complexes after the addition of GroES oligomers, but it precluded the subsequent association of a second GroES oligomer under conditions that otherwise would promote the efficient formation of symmetrical chaperonin complexes. This observation and the instability of the symmetrical particles in the presence of ATP explains why conditions that allow the binding of two GroES per GroEL oligomer can be compatible with chaperonin-mediated protein folding (24). A kinetic analysis of the nucleotide-dependent interaction between GroEL and GroES also demonstrates that the distinct steps of the chaperonin reaction cycle can be explained on the basis of the asymmetrical chaperonin complex alone (27).

REFERENCES AND NOTES

1. S. J. Landry and L. M. Gierasch, *Annu. Rev. Biomol. Struct.* **23**, 645 (1994); J. P. Hendrick and F. U. Hartl, *Annu. Rev. Biochem.* **62**, 349 (1993); M.-J. Gething and J. Sambrook, *Nature* **355**, 33 (1992); R. J. Ellis and S. M. van der Vies, *Annu. Rev. Biochem.* **60**, 321 (1991).
2. T. Hohn, B. Hohn, A. Engel, M. Wurtz, P. R. Smith, *J. Mol. Biol.* **129**, 359 (1979); R. W. Hendrix, *ibid.*, p. 375.
3. H. R. Saibil et al., *Curr. Biol.* **3**, 265 (1993).
4. T. Langer, G. Pfeifer, J. Martin, W. Baumeister, F. U. Hartl, *EMBO J.* **11**, 4757 (1992).
5. S. Chen et al., *Nature* **371**, 261 (1994).
6. K. Braig et al., *ibid.*, p. 578.
7. K. Braig, M. Simon, F. Furuya, J. F. Hainfeld, A. L. Horwich, *Proc. Natl. Acad. Sci. U.S.A.* **90**, 3978 (1993).
8. W. A. Fenton, V. Kashi, K. Furtak, A. L. Horwich, *Nature* **371**, 614 (1994).
9. P. V. Viitanen et al., *Biochemistry* **29**, 5664 (1990).
10. J. Martin et al., *Nature* **352**, 36 (1991).
11. S. J. Landry, J. Zeilstra-Ryalls, O. Fayet, C. Georgopoulos, L. M. Gierasch, *ibid.* **364**, 255 (1993).
12. T. E. Gray and A. R. Fersht, *FEBS Lett.* **292**, 254 (1991); E. S. Bochkareva and A. S. Girshovich, *J. Biol. Chem.* **267**, 25672 (1992).
13. G. S. Jackson et al., *Biochemistry* **32**, 2554 (1993).
14. J. Martin, M. Mayhew, T. Langer, F. U. Hartl, *Nature* **366**, 288 (1993).
15. A. Azem, M. Kessel, P. Goloubinoff, *Science* **265**, 653 (1994).
16. M. J. Todd, P. V. Viitanen, G. H. Lorimer, *Biochemistry* **32**, 8560 (1993).
17. T. E. Creighton, *Nature* **352**, 17 (1991).
18. H. R. Saibil, D. Zheng, S. Wood, A. auf der Mauer, *ibid.* **353**, 25 (1991).
19. O. Llorca, S. Marco, J. L. Carrascosa, J. M. Valpuesta, *FEBS Lett.* **345**, 181 (1994).
20. M. Schmidt et al., *Science* **265**, 656 (1994).
21. Glutaraldehyde cross-linking under mild conditions (Fig. 1, legend) preserved the association between GroEL and GroES during negative staining or desalting prior to scanning transmission electron microscopy. The results of control incubations of GroEL and GroES with the nonhydrolyzable ATP analog

AMP-PNP, followed by cross-linking and electron microscopic analysis, were compared with a biochemical binding analysis by equilibrium dialysis, omitting the cross-linking step (Fig. 2). The comparison showed that glutaraldehyde cross-linking under the conditions used in this study measures the occurrence of GroEL:GroES and GroEL:(GroES)$_2$ particles reliably.

22. J. Frank, J. P. Bretaudiere, J. M. Carazo, A. Verschoor, T. Wagenknecht, *J. Microsc.* **150**, 99 (1988).
23. S. Müller, K. N. Goldie, R. Bürki, R. Häring, A. Engel, *Ultramicroscopy* **46**, 317 (1992).
24. According to Azem *et al.* (*15*), 3.5 μM ATP is sufficient for half-maximal formation of GroEL:GroES complexes in the absence of substrate protein, whereas ~400 μM ATP is necessary for the assembly of GroEL:(GroES)$_2$ particles under the appropriate buffer conditions. We found that a constant concentration of 15 μM ATP is required for GroES binding to occur at the half-maximal rate (*27*). Analysis of the dependence of GroEL- and GroES-mediated folding of bovine rhodanese (*4, 10, 14*) on the ATP concentration showed that half-maximal folding activity is achieved at 50 to 100 μM ATP. Significant renaturation is apparent already at 20 μM ATP. The yield of refolding was 20 to 30% higher at 5 mM Mg^{2+} and pH 7.2 than at 50 mM Mg^{2+} and pH 8.0, at which a large fraction of chaperonin complexes are symmetrical in the absence of substrate protein.
25. [^{3}H]GroES was fully functional in chaperonin-mediated protein folding (*4*).
26. M. J. Todd, P. V. Viitanen, G. H. Lorimer, *Science* **265**, 659 (1994).
27. M. K. Hayer-Hartl, J. Martin, F. U. Hartl, *ibid.* **269**, 836 (1995).
28. 6His-N-DHFR is a construct derived from mouse DHFR and contains the sequence Met-His$_6$-Gly-Cys-Gly joined to the NH$_2$-terminus of DHFR by a factor X cleavage site.
29. Unfolded rhodanese was diluted 100-fold to 0.18 μM from 6 M guanidinium chloride and 5 mM dithiothreitol into a solution of 60 nM GroEL in 50 mM tris-HCl (pH 8.0), 50 mM KCl, and 50 mM magnesium acetate. Aggregates were removed by centrifugation and GroES binding to the rhodanese:GroEL complex in the supernatant fraction was measured as in Fig. 2C. Control reactions lacking rhodanese contained an equivalent concentration of guanidinium chloride.
30. It was shown that GroEL can be cross-linked to a folding intermediate of ribulose-1,5-bisphosphate carboxylase-oxygenase (RuBisCO I) and two GroES oligomers, suggesting that substrate polypeptide binds to the outer surface of GroEL (*15*). Such cross-linking, detected by polyacrylamide electrophoresis in tube gels, may indeed have occurred during the extensive incubation of the protein mixture (60 min) with high concentrations of glutaraldehyde at 37°C (*15*). It may be important in this context that RuBisCO I, after dilution from denaturant, aggregates slowly and is potentially available for cross-linking for long periods of time (*26*). In the present study, GroEL:(GroES)$_2$ complexes were not observed in the presence of unfolded proteins with mild glutaraldehyde cross-linking (*21*) and electron microscopy.
31. Studies describing the formation of GroEL:(GroES)$_2$ particles used reaction buffers containing 15 to 50 mM Mg^{2+} at pH 7.5 to 8.0 (*15, 19, 20*). The free Mg^{2+} concentration in the cell is only 1 to 2 mM (*32*) at a total concentration of 10 to 20 mM. At 20 mM free Mg^{2+} and pH 7.5 (*15*) and in the presence of AMP-PNP, ~30 to 50% of GroEL bound two GroES oligomers, as measured by size-exclusion chromatography. At 50 mM Mg^{2+} and pH 8.0 (*20*), close to 100% of GroEL bound two GroES oligomers (Figs. 2 and 3).
32. T. Alatossava, H. Jutte, A. Kuhn, E. Kellenberger, *J. Bacteriol.* **162**, 413 (1985).
33. A. Bremer, C. Henn, A. Engel, W. Baumeister, U. Aebi, *Ultramicroscopy* **46**, 85 (1992).
34. We thank J. Martin for performing the rhodanese refolding experiments. Supported by NIH grant GM 50908, the Swiss National Foundation for Scientific Research (grant 31-32536.91), and the M. E. Müller Foundation of Switzerland.

4 April 1995; accepted 16 June 1995

Asymmetrical Interaction of GroEL and GroES in the ATPase Cycle of Assisted Protein Folding

Manajit K. Hayer-Hartl, Jörg Martin, F. Ulrich Hartl*

The chaperonins GroEL and GroES of *Escherichia coli* facilitate protein folding in an adenosine triphosphate (ATP)–dependent reaction cycle. The kinetic parameters for the formation and dissociation of GroEL-GroES complexes were analyzed by surface plasmon resonance. Association of GroES and subsequent ATP hydrolysis in the interacting GroEL toroid resulted in the formation of a stable GroEL:ADP:GroES complex. The complex dissociated as a result of ATP hydrolysis in the opposite GroEL toroid, without formation of a symmetrical GroEL:(GroES)$_2$ intermediate. Dissociation was accelerated by the addition of unfolded polypeptide. Thus, the functional chaperonin unit is an asymmetrical GroEL:GroES complex, and substrate protein plays an active role in modulating the chaperonin reaction cycle.

The chaperonins mediate protein folding in the cell by preventing the formation of unproductive associations within and between nonnative polypeptides (*1–3*). GroEL, the chaperonin in *E. coli* cytosol, is a large oligomeric complex composed of two stacked heptameric rings of identical ~58-kD subunits that form a central cavity (*4, 5*). Studies indicate that GroEL binds one molecule of substrate protein within this cavity in a conformation resembling the molten globule (*3, 4, 6–8*). Folding is achieved through cycles of protein release and rebinding that are dependent on ATP hydrolysis (*3, 9*) and regulated by GroES, a single heptameric ring of ~10-kD subunits (*3, 10–12*). Asymmetrical binding of GroES to one end of the GroEL cylinder has been proposed to be a key feature of the reaction, leaving the cavity of one toroid available for the association of substrate protein (*4*). GroES binding is nucleotide-dependent and is thought to exert a negative cooperative effect, preventing the association of a second GroES oligomer with the opposite GroEL toroid (*4, 13*). GroES increases the cooperativity of the GroEL adenosine triphosphatase (ATPase) (*12, 14–16*) and, after ATP hydrolysis, stabilizes the seven interacting GroEL subunits in the adenosine diphosphate (ADP)–bound state (*15*). As a result, the GroEL ATPase is inhibited by 50% (*10*). GroES dissociates after ATP hydrolysis in the uninhibited GroEL toroid (*15, 17*); its association (or reassociation) with a substrate:GroEL complex results in ATP-dependent protein release for folding.

Recently, the electron microscopic observation of symmetrical GroEL:(GroES)$_2$ complexes (*18–20*) has led to several new proposals that differ from the model of chaperonin action outlined above: (i) The symmetrical chaperonin particle was invoked as an obligatory intermediate preceding the step of ATP hydrolysis in the reaction that results in GroES release (*17, 20*). (ii) Substrate protein was proposed to interact with the outer surface of the chaperonin cylinder because symmetrical binding of GroES would prevent access to the GroEL cavity (*19*). (iii) The interaction between GroEL and GroES was claimed to be independent of substrate protein (*17*). We have now analyzed the steps of the chaperonin reaction cycle with kinetic and biochemical methods that allowed us to distinguish between a functional stoichiometry for GroEL:GroES of 1:1 or 1:2.

Complex formation between GroEL and GroES as a function of nucleotide binding was analyzed by surface plasmon resonance (SPR). This technique measures the real-time association and dissociation of protein molecules on a sensor surface and allows precise and highly reproducible estimates of kinetic binding constants (*21*). The kinetic properties of the GroEL-GroES interaction were compared under various conditions. Either GroEL or GroES was functionally immobilized to the sensor surface of the flow cell. Efficient complex formation occurred in the presence of adenine nucleotide and Mg^{2+} (Fig. 1) (*22*). Similar binding parameters were obtained irrespective of whether GroEL or GroES was immobilized (Fig. 1 and Table 1). Thus, covalent coupling to the flow cell per se did not affect the functional properties of these proteins (*23*). SPR response curves for the ADP-dependent binding of increasing concentrations of GroEL to immobilized GroES are shown in Fig. 1A. Association occurred in a monophasic reaction with an apparent rate constant, k_a, of ~4 × 10^5 M^{-1} s^{-1} (Table 1). Association may be slower than that in free solution because of the motional restraint of one of the partner molecules. The rate of complex formation in the presence of ATP was approximately three times that in the presence of ADP (Fig. 1B and Table